IEEE Transactions on Terahertz Science and Technology

Temporal and spatial variability of water status in plant leaves by terahertz imaging

Journal:	*Transactions on Terahertz Science and Technology*
Manuscript ID	xxxxxxxxxxxxxxxxxxxxxxxxxx
Manuscript Type:	Regular Paper
Date Submitted by the Author:	14-May-2018
Complete List of Authors:	Song, Zheyu; Changchun University of Science and Technology, School of Optoelectronic Engineering; Chongqing Institute of Green and Intelligent Technology, Chongqing Key Laboratory of Multi-scale Manufacturing Technology Yan, Shihan; Chongqing Institute of Green and Intelligent Technology, Chongqing Key Laboratory of Multi-scale Manufacturing Technology Zang, Ziyi; Jilin University, College of Instrumentation & Electrical Engineering; Chongqing Institute of Green and Intelligent Technology, Chinese Academy of Sciences, Chongqing Key laboratory of Multi-Scale manufacturing Technology Fu, Yun; Changchun University of Science and Technology, School of Optoelectronic Engineering Wei, Dongshan; Chongqing Institute of Green and Intelligent Technology, Chinese Academy of Sciences; Dongguan University of Technology, School of Electronic Engineering Cui, Hongliang Lai, Puxiang; Hong Kong Polytechnic University, Department of Biomedical Engineering
TOPIC AREA FOR SUBMISSION :	THz applications in biology and medicine

Temporal and spatial variability of water status in plant leaves by terahertz imaging

Zheyu Song[1, 2, #], Shihan Yan[2, #], Ziyi Zang[2, 3], Yun Fu[1,*], Dongshan Wei[2, 4, *], Hong-Liang Cui[2, 3], and Puxiang Lai[5]

[1] School of Optoelectronic Engineering, Changchun University of Science and Technology, Changchun, Jilin, 130022, China.

[2] Chongqing Engineering Research Center of High-Resolution and Three-Dimensional Dynamic Imaging Technology, Chongqing Institute of Green and Intelligent Technology, Chinese Academy of Sciences, Chongqing, 400714, China.

[3] College of Instrumentation & Electrical Engineering, Jilin University, Changchun, Jilin, 130061, China.

[4] School of Electronic Engineering, Dongguan University of Technology, Dongguan, Guangdong, 523808, China.

[5] Department of Biomedical Engineering, Hong Kong Polytechnic University, Hong Kong

[#] These authors contributed equally to this research.

* To whom correspondence should be addressed: linda_fy@cust.edu.cn, dswei@dgut.edu.cn.

Abstract: Water and its distribution and transport dynamics in green plant leaves are vital to the growth of plants. Owing to the high sensitivity of terahertz (THz) wave to water, THz spectroscopy has great advantages in analyzing the water status of plant leaves. This paper presents a new approach to estimate the water status of plant leaves by the THz time-domain spectroscopy (THz-TDS) technique. Spatial distribution of THz transmission amplitudes located in vein xylem and mesophyll of all three kinds of leaves including wintersweet, ginkgo and bamboo is detected by THz-TDS measurements. Based on the transmission amplitude, the reconstructed THz images show that the water loss in the basal leaf region is more than that in the distal region during the natural drying process for all three plants. A good agreement is reached between the THz imaging method and the direct water weight measurement. To illustrate the accuracy and the sensitivity of the THz technique, the temporal and spatial variations of the water content in the damaged ginkgo leaf with a wound by cutting are also investigated for comparison. The water flow from the basal region to the distal region of the leaf is inferred according to the variation of THz transmission amplitude with the leaf region in different dehydration periods, which is consistent with the string-of-lakes model prediction. This work shows the feasibility of using THz technology to monitor the temporal and spatial variability of the water status in plant

leaves.

Key words: terahertz, plant leaf, imaging, water content, spatial variability, dehydration

I. INTRODUCTION

Water is a fundamental chemical constituent in plants and its content in vegetative tissues is a parameter of high importance to plant science. Water abundance in leaves is closely influenced by the leaf vigor and phylogenic traits such as the leaf structure, the shape and the photosynthetic efficiency [1, 2]. The heterogeneous change of water content in leaves and the distribution and kinetics of water in plant tissues have been proved to be affected by many factors such as environmental stresses [3], diseases [4] andgrowth rhythm [5]. There are three representative leaf water models: two-pool model, Pe´clet effect, and string-of-lakes to describe the water status in plant leaves [1]. All these models can be used to describe the potential kinetics of water in leaves, but none can well account for the leaf water enrichment mechanism [1]. Describing the water spatial variability of plant leaves in detail can clearly indicate different capacities of plants to mobilize water between different mesophyll and venation parts of the leaf. It will also improve the criteria as to what parts of the leaf are the most appropriate for conducting physiological measurements at different metabolic states or environmental pressures, and will help understand the water enrichment mechanism in leaves [6].

Many imaging techniques, such as thermal imaging [7], near infrared imaging [8], hyperspectral imaging [9] and ^{1}H magnetic resonance imaging (MRI) [6], have been proposed to provide visualization and analyses of detailed spectral and spatial information of water status in plant leaves, which have significantly advanced the plant physiology research. However, each of these techniques has its own limitations. For example, thermal imaging and hyperspectral imaging are usually classified as derivation methods, which reflect the comprehensive influence caused by the change of water content [7, 10]. Relying on the infrared or microwave spectrum, they either lack sensitivity to minor changes in water status in leaves, or are affected by the inorganic salt content of the plant, leading to significant disturbances in measurement [11]. Moreover, the imaging resolution based on the microwave radiation is confined to the minimal wavelength of approximately 2.5 mm. The MRI imaging shows higher resolution, but it is costly and its accessibility is limited [12].

Evolving measurement techniques based on the terahertz (THz) electromagnetic radiation, extending from approximately 100 GHz to 10 THz have shown unique advantages in monitoring minute changes of the water content due to the high sensitivity of THz radiation to water [13]. Furthermore, THz techniques do not bring additional environmental impacts caused by ionizing radiation because of its low photon energy. Thus, a growing attention in the plant physiology has been

directed to THz spectroscopy techniques [14-18], as a non-invasive tool for measuring leaf water status [13, 19] under certain conditions such as drought stress [20, 21] and dehydration kinetics [22]. However, hitherto only a few researches have involved THz imaging to explore the organizational heterogeneity in the field of botany [23, 24]. Compared with the spectroscopy, imaging can actually provide more details about the spectral, temporal, and spatial variability [15]. Visualized description of the spatial heterogeneity in distribution and kinetics of the leaf water status across the leaf surface [25] can deepen our understanding of the complex traits related to the growth, yield and adaptation to biotic or abiotic stress (disease, insects, drought and salinity) for dissecting the metabolic processes of different leaf areas and tissues [26].

The absorption and dispersion coefficients, refractive index and other physical parameters can be employed as the signals of pixels to perform THz imaging [27]. Previously, THz imaging has been proved to be a useful complementary technology for nondestructive testing [28]. Objectively speaking, however, THz imaging is not advantageous enough due to the relative low spatial resolution resulting from its long wavelength from 30 μm to 3 mm generally accepted. Particularly, the far-field spatial resolution of THz imaging is restricted to the Rayleigh criterion which corresponds to 180 μm in vacuum at 1 THz [29]. Luckily, the size of plant leaves in centimeter is much larger than this scale. Besides, typical accuracy of ~100 μm can be achieved by improving the image processing schemes of the THz time-domain spectroscopy (THz-TDS) system [30]. Thus, the recent developments of sensitive THz imaging platforms and precise image processing schemes have opened up the possibility toward high-resolution studies on water variation of plant leaves and the related kinetics [8].

This paper illustrates the use of THz imaging as a flexible and powerful platform to study the temporal and spatial variations of water status in three kinds of plant leaves with typical venations. The temporal and spatial changes of water content in the whole leaf and different leaf regions are investigated by THz imaging based on semi-quantitative THz image signals. A strong correlation is identified between the THz imaging and the conventional water weight measurement, demonstrating the feasibility of this method for monitoring the temporal and spatial variability of leaf water content. In addition, *in situ* detection also can be achieved *in vivo* by adjusting the scanning operation shelf of the THz imaging system.

II. EXPERIMENTAL SECTION

A. Leaf samples

Three kinds of fresh leaves of wintersweet (*Chimonanthus praecox*), ginkgo (*Ginkgo biloba*) and bamboo (*Bambusa multiplex*) cultivated in Chongqing Institute of Green and Intelligent Technology, Chinese Academy of Sciences were picked and shown in Fig. 1. These fresh leaves were first used for THz imaging, and then weighed by an accurate electronic balance. Each of these leaves was tested individually and repeatedly every day at the same time under the same conditions during seven successive days. The tested environment temperature was 22 °C ± 0.1 °C and the humidity was 50% ± 2%.

B. Setup of the THz imaging system

The THz imaging system used in experiment was based on the THz time-domain spectroscopy system (T-Ray 5000) produced by Advanced Phonotix, Inc. (API). The schematic diagram of the whole system in transmission mode is shown in Fig. 2a, which had been described in detail in our previous work [30, 31]. Fig. 2b shows the measured sample fixed on the XY two-dimensional moving stage. The transparent holder for the sample is made of polyethylene with low absorption in the terahertz frequency band. The raster scanning step size is 0.25 mm and the scanning speed is 50 mm/sec, i.e., the dwell time at each pixel is 5 ms, longer than the spectral scanning time of 1 ms of the THz system. The imaging areas of the XY-stage are 10.4 cm × 6.3 cm for wintersweet, 6 cm × 7.5 cm for ginkgo, and 10.5 cm × 3.1 cm for bamboo, respectively.

C. THz imaging

By collecting, analyzing and reconstituting the THz transmission spectrum data, the two-dimensional image of the sample containing all areas of the leaf is obtained. For the time-domain imaging, each pixel in the image corresponds to the signal waveform of THz pulse in time-domain on one certain point of the leaf. THz time-domain spectral imaging can reflect the obviously enhanced contrast difference [27]. While the frequency-domain pattern imaging based on the absorption coefficient, dispersive coefficient, refractive index or other physical parameters of each pixel can usually yield a relatively better imaging result [32]. Imaging resolution increases with the frequency, but on the other hand, the penetration depth of the THz radiation decreases, leading to a decreased signal-to-noise ratio. Therefore, the choice of imaging frequencies needs to be tested to get a trade-off

compromise between the two constraints [33].

THz frequency-domain imaging of the leaf is obtained according to the following expression:

$$a_{(x,y)}=abs(F_{sam(x,y)}(\omega))/abs(F_{ref}(\omega)) \quad (1)$$

where $a_{(x,y)}$ is the value of each pixel in the two-dimentional THz frequency-domain imaging, *i.e.*, the pixel information, $abs(F_{sam(x,y)}(\omega))$ is the transmission amplitude after Fourier transform of the sample at each pixel , and $abs(F_{ref}(\omega))$ is the that of the reference (air) at the same frequency under the same conditions.

D. Statistical analyses

The water status of the leaf relative to the first day is calculated as,

$$LWS(\%)=\frac{w_n}{w_1}\times 100\% \quad (2)$$

where w_1 means the weight of the fresh leaf at the first day and w_n means the weight in one of the seven successive days.

In previous work [20, 22], the THz transmission was extracted as the signal to explore the water content of the leaves. Without any absorbing or reflecting materials, the transmission is defined as 100%, i.e. the THz transmission of air is used as a standard [20]. Since the THz transmission is reversely proportional to water content due to the high absorption coefficient of water, there is an opposite trend between the increasing THz transmission amplitude and the decreasing water content of the leaf. For the convenience of discussion, in this work, we keep the numerical THz image signals to have the same trend with the water content of leaves. Therefore, the THz image signals is defined in reverse proportion to the THz transmission amplitude for investigating the dehydration kinetics of leaves. To be consistent with the definition of the leaf water status as Eq. 2, the THz image signal (T) of the leaf is defined as,

$$T(\%)=\frac{a_1}{a_n}\times 100\% \quad (3)$$

where a_1 means the pixel information (Eq. 1) of the sample on the first day and a_n means the pixel information on one of the seven successive days at the same location. The pixel information for THz imaging is collected and averaged from a serial of pixels at the same spatial location on each day during the water loss process.

In order to examine whether THz imaging has the ability to explore the spatial distribution of water at different regions of the leaf, we compare the THz image signals at different locations on the

mesophyll and vein, and at least 20 independent points were chosen respectively. The definite basal, intermediate and distal regions on the leaf are determined referred to the previous study [6]. Correlation between the gravimetric water content and the THz image signals of each measured leaf is successively analyzed by Pearson correlation coefficient.

III. RESULTS AND DISCUSSION

A. Determine the optimal imaging frequency for each plant

The THz time-domain waveforms were measured for every pixel during the imaging procedure. Fig 3a is plotted by the peak-to-peak feature of the time-domain waveform imaging. Figs. 3b, c and d were plotted by the THz transmission amplitude at fixed frequency points of 0.6, 0.89 and 1.15 THz, respectively. Vein outline in the frequency-domain image with anyone of the three frequencies, shows a much clearer structure compared with that in the time-domain imaging (Fig. 3a). The frequency-domain images with higher frequencies reflect obviously more elaborate structure in the leaf tissue. The electromagnetic beams converge more as the frequencies of the beams increase and thus the resolution increases, so the veins has a much clearer outline in higher frequencies [34-36]. But meanwhile, the absorption coefficient also increases with the increase of the frequency, causing the penetration depth of THz beams and the signal-to-noise ratio to decrease [37]. Thus, there are different colors of the backgrounds in Figs. 3b-d, representing different THz transmission amplitudes of the sample holder at different frequencies. With the increase of the imaging frequency, the background signal decreases as shown in Figs. 3b-d. The imaging result at 0.89 THz achieves a trade-off between the appropriate imaging resolution and the good signal-to-noise ratio.

B. Temporal and spatial variations of water content in leaves

The optimal imaging frequencies are 0.89 THz for wintersweet, 0.85 THz for ginkgo and 0.9 THz for bamboo, respectively, since the thickness difference and the component diversity of these three plant leaf samples give rise to different optimal frequencies [38]. During the entire drying process of the leaf, THz image signals representing the reverse of the transmission amplitude of every plant leaf decrease significantly, which indicates the water loss process of the leaves (Fig. 4). The THz image of the wintersweet leaf exhibits an obvious reticulate venation and a heterogeneous patch between mesophyll and vein, which reflects the spatial variability of the leaf water status(Fig. 4a). However, the boundary is blurred and the demarcation lines drawing the outline of the venation are vague in shape,

which makes the dichotomous venation of ginkgo and the parallel venation of bamboo not easy to be observed because of their thinner veins compared to that of the wintersweet, and leads to a consequent relatively low resolution in millimeter scale [39]. The THz imaging method allows for the detection of the spatial variability of the leaf water status among distal, intermediate and basal leaf regions over time, because of the large absorption coefficient of water [40] and the relatively small absorption coefficient of the dry-matter leaf [17, 41]. It is noteworthy that in Figs. 4a and b, there are weak fringes in the background. These fringes similar to the Newton ring are caused by the interference phenomenon due to the reflections of the uneven surface of the leaf and the flat plastic holder. These undesired fringes can be effectively removed using an appropriate imaging algorithm, but it is not involved in the present work.

Furthermore, to quantitatively describe the temporal and spatial variability of the leaf water status, exact numerical values extracted from these images were used. The THz image signals of wintersweet and ginkgo decrease almost linearly, while that of the bamboo leaf decreases in a nonlinear form with the increase of the dehydration days (Fig 5). Unlike the wintersweet and ginkgo, the mesophyll cells of bamboo do not differentiate palisade and spongy tissues [42, 43] and they are irregularly shaped cells that have many well-developed intercellular spaces that allow the passage of gases [44], therefore the water loss rate of bamboo is slower than those of the wintersweet and ginkgo, especially in the later dehydration days. Comparing with the ginkgo leaf, there is a relatively higher dehydration rate for the wintersweet leaf during the first three days (Figs. 5a and b), because the ginkgo leaf has a waxy protective layer on the surface, which can retard the evaporation of water from the leaf surface [45]. More detailed comparison of the difference between the mesophyll and vein parts based on the THz image signals of the wintersweet leaf shows the water reduction is greater in leaf veins than that in leaf parenchyma parts (Fig. 6). In addition, the THz image signals gradually decrease along the distal, intermediate and basal regions on the same dehydration day (Fig. 6), indicating the rate of water loss in the basal region is higher, which is in good agreement with the previous report [6].

C. Correlation analysis of different measurement methods for each plant leaf

The response of photosynthesis and respiration can affect the process of metabolism, which is related to the productivity of plants [46]. Using THz imaging for crop water status monitoring helps grasp the growth of plants at different stages, avoid irreversible damage, and thus substantially reduce

or prevent yield losses [47]. In addition, the water loss rate of leaves *in vitro* have been proved to be used as one of the physiological indices for drought resistance evaluation [48]. Therefore in this work, in order to test the reliability and applicability of the method, the water content was also measured through a traditional weighing method (Fig.7). Here, the correlation analyses were performed to test the consistency of results obtained by different methods. From the Pearson analysis results, the correlation coefficients of the three leaves are 0.996 (wintersweet, Fig. 8a), 0.991 (ginkgo, Fig. 8b) and 0.993 (bamboo, Fig. 8c), respectively. The results indicate that there is a strong linear positive correlation between the THz image signal and the water content measured by the conventional weighing method regardless of the kinds of leaves. The Pearson correlation coefficients suggest that the THz imaging can be well used to detect the temporal and spatial variability of the water status of plant leaves among different tissues and different parts of leaves.

D. Influence of the wound on the dehydration kinetics of the ginkgo leaf

Water transport in the plant leaf is a key and important problem for the leaf growth. To look into the water transport in the leaf, a knife cut near the basal region of the ginkgo leaf was performed to obtain a damaged leaf with a wound. Data of THz transmission amplitudes extracted from Fig. 4b at thirteen different locations ranging from the distal to the basal regions along the veins for the control and damaged ginkgo leaves on the first and seventh days are compared in Fig. 9. As seen from Fig. 9, the transmission amplitude at the distal region is higher than that at the basal region for all curves, confirming the above finding that the water content in the basal region is higher than that in the distal region of the leaf. For the control leaf, the increase of the transmission amplitude from the first day to the seventh day at the basal region is slightly higher than that at the distal region, indicating more water loss at the basal region, which confirms our above finding and agrees well with the report in Ref. 6. While for the damaged ginkgo leaf, the transmission amplitude has a distinct increase on the seventh day around the ninth location, the same position to the knife cut, indicating the accuracy and the sensitivity of the THz technique. Furthermore, the THz transmission amplitude becomes higher at the distal and intermediate regions and almost keeps unchanged at the basal region comparing with the control leaf on the seventh day. This may indicate there is a water flow from the basal region to the distal region for the control leaf and the water supply is cut off for the damaged leaf, resulting in the water loss at the distal and intermediate regions in a more serious degree. The water flow direction

inferred by the THz technique is in agreement with the prediction from the string-of-lakes model [1].

IV. CONCLUSIONS

In summary, we proposed a quantitative method to evaluate the water content of plant leaves by the THz imaging technique. We used the THz-TDS imaging system to examine the water content of leaves and studied the relationship between the water content and the THz image signals. By THz imaging, changes of the water content and the water distribution in a plant leaf could be determined. The significance of the work lies in the systematic application of THz imaging technology to monitor the dehydration kinetics of leaves from different regions of the leaf and different plant species. The good agreement between the THz image signal and the weight measurement suggests that THz imaging has a good potential to measure the water content of plant leaves in a simple, fast, and label-free way. More structure details of the margin, intercostal, venous and basal mesophyll and vein of pleat leaves can be detected by THz technique if the imaging enhancement processing is performed or by combining THz imaging with the photoacoustic imaging [49,50], which will be our future work directions.

ACKNOWLEDGMENTS

This work is part supported by the National Key R&D Program of China (2016YFC0101300, 2017YFF0106303 and 2016YFC0101002), National 973 Program of China (2015CB755401), national natural science foundation of China (11504372, 61605206 and 61771138) and Dongguan Industry University Research Cooperation Project (2015509102211).

References:

[1] K. S. Gan, S. C. Wong, J. W. H. Yong, and G. D. Farquhar, "18O Spatial Patterns of Vein Xylem Water, Leaf Water, and Dry Matter in Cotton Leaves," *Plant Physiology,* vol. 130, pp. 1008-1021, 2002.

[2] P. J. Kramer and J. S. Boyer, "Water relations of plants and soils," *Water Relations of Plants & Soils,* 2014.

[3] S. Bhattacharjee and A. K. Saha, "Plant Water-Stress Response Mechanisms," *Approaches to Plant Stress & Their Management,* pp. 149-172, 2014.

[4] F. Workneh, J. A. Price, D. C. Jones, and C. M. Rush, "Wheat Streak Mosaic: A Classic Case of Plant Disease Impact on Soil Water Content and Crop Water-Use Efficiency," *Plant Disease An International Journal of Applied Plant Pathology,* vol. 94, pp. 771-774, 2010.

[5] I. C. Buchanan-Bollig and J. A. C. Smith, "Circadian rhythms in crassulacean acid metabolism: phase relationships between gas exchange, leaf water relations and malate metabolism in *Kalanchoë daigremontiana*," *Planta,* vol. 161, pp. 314-319, 1984.

[6] S. Jordi, P. Josep, and L. P. Silvia, "Changes in water content and distribution in Quercus ilex leaves during progressive drought assessed by in vivo 1H magnetic resonance imaging," *BMC Plant Biology,* vol. 10, p. 188, 2010.

[7] O. M. Grant, H. Ochagavía, J. Baluja, M. P. Diago, and J. Tardáguila, "Thermal imaging to detect spatial and temporal variation in the water status of grapevine (*Vitis vinifera* L.)," *Journal of Horticultural Science & Biotechnology,* vol. 91, pp. 44-55, 2016.

[8] S. Higa, H. Kobori, and S. Tsuchikawa, "Mapping of leaf water content using near-infrared hyperspectral imaging," *Applied Spectroscopy,* vol. 67, pp. 1302-1307, 2013.

[9] M. P. Diago, A. Pou, B. Millan, J. Tardaguila, A. M. Fernandes, and P. Melopinto, "Assessment of grapevine water status from hyperspectral imaging of leaves," *Acta Horticulturae,* vol. 1038, pp. 89-96, 2014.

[10] E. Achata, C. Esquerre, C. O'Donnell, and A. Gowen, "A study on the application of near infrared hyperspectral chemical imaging for monitoring moisture content and water activity in low moisture systems," *Molecules,* vol. 20, pp. 2611-2621, 2015.

[11] F. T. Ulaby and R. P. Jedlicka, "Microwave Dielectric Properties of Plant Materials," *IEEE Transactions on Geoscience & Remote Sensing,* vol. GE-22, pp. 406-415, 1984.

[12] M. Sarracanie, C. D. Lapierre, N. Salameh, D. E. J. Waddington, T. Witzel, and M. S. Rosen, "Low-Cost High-Performance MRI," *Scientific Reports,* vol. 5, p. 15177, 2015.

[13] R. Gente and M. Koch, "Monitoring leaf water content with THz and sub-THz waves," *Plant Methods,* vol. 11, p. 15, 2015.

[14] B. Breitenstein, M. Scheller, M. K. Shakfa, T. Kinder, M. Koch, D. Selmar*, et al.*, "Introducing terahertz technology into plant biology: A novel method to monitor changes in leaf water status," *Journal of Applied Botany & Food Quality,* vol. 84, pp. 158-161, 2012.

[15] W. L. Chan, J. Deibel, and D. M. Mittleman, "Imaging with terahertz radiation," *Reports on Progress in Physics,* vol. 70, pp. 1325-1379, 2007.

[16] S. Hadjiloucas, L. S. Karatzas, and J. W. Bowen, "Measurements of leaf water content using terahertz radiation," *IEEE Transactions on Microwave Theory & Techniques,* vol. 47, pp. 142-149, 1999.

[17] B. B. Hu and M. C. Nuss, "Imaging with terahertz waves," *Optics Letters,* vol. 20, pp. 1716-1718, 1995.

[18] P. U. Jepsen, D. G. Cooke, and M. Koch, "Terahertz spectroscopy and imaging – Modern techniques and applications," *Laser & Photonics Reviews,* vol. 5, pp. 418-418, 2011.

[19] R. U. S. De Cumis, J. H. Xu, L. Masini, R. Degl'Innocenti, P. Pingue, P. A. Benedetti*, et al.*, "Terahertz confocal microscopy with a quantum cascade laser source," *Optics Express,* vol. 20, pp. 21924-21931, 2012.

[20] N. Born and M. Koch, "Monitoring plant drought stress response using terahertz time-domain spectroscopy," *Plant Physiology,* vol. 164, pp. 1571-1577, 2014.

[21] C. Jördens, M. Scheller, B. Breitenstein, D. Selmar, and M. Koch, "Evaluation of leaf water status by means of permittivity at terahertz frequencies," *Journal of Biological Physics,* vol. 35, pp. 255-264, 2009.

[22] E. Castrocamus, M. Palomar, and A. A. Covarrubias, "Leaf water dynamics of Arabidopsis thaliana monitored in-vivo using terahertz time-domain spectroscopy," *Scientific Reports,* vol. 3, p. 2910, 2013.

[23] H. Qin, J. Sun, Z. He, X. Li, X. Li, S. Liang, *et al.*, "Heterodyne detection at 216, 432, and 648GHz based on bilayer graphene field-effect transistor with quasi-optical coupling," *Carbon,* vol. 121, pp. 235-241, 2017.

[24] H. Qin, J. Sun, S. Liang, X. Li, X. Yang, Z. He, *et al.*, "Room-temperature, low-impedance and high-sensitivity terahertz direct detector based on bilayer graphene field-effect transistor," *Carbon,* vol. 116, pp. 760-765, 2017.

[25] L. Shuai, Y. J. Zhang, S. Lawren, S. Christine, I. Atsushi, Y. J. Chen, *et al.*, "The Heterogeneity and Spatial Patterning of Structure and Physiology across the Leaf Surface in Giant Leaves ofAlocasia macrorrhiza," *Plos One,* vol. 8, p. e66016, 2013.

[26] L. Li, Q. Zhang, and D. Huang, "A Review of Imaging Techniques for Plant Phenotyping," *Sensors,* vol. 14, pp. 20078-20111, 2014.

[27] L. Xing, H. L. Cui, C. Shi, T. Chang, D. Wei, C. Du, *et al.*, "Void and crack detection of polymethacrylimide foams based on terahertz time-domain spectroscopic imaging," *Journal of Sandwich Structures & Materials,* vol. 19, pp. 348–363, 2016.

[28] J. Zhang, C. Shi, Y. Ma, X. Han, W. Li, T. Chang, *et al.*, "Spectroscopic study of terahertz reflection and transmission properties of carbon-fiber-reinforced plastic composites," *Optical Engineering,* vol. 54, p. 54106, 2015.

[29] F. Blanchard, A. Doi, T. Tanaka, H. Hirori, H. Tanaka, Y. Kadoya, *et al.*, "Real-time terahertz near-field microscope," *Optics Express,* vol. 19, pp. 8277-8284, 2011.

[30] L. Xing, H. L. Cui, C. Shi, Z. Zhang, J. Zhang, T. Chang, *et al.*, "Nondestructive examination of polymethacrylimide composite structures with terahertz time-domain spectroscopy," *Polymer Testing,* vol. 57, pp. 141-148, 2017.

[31] S. Yan, D. Wei, M. Tang, C. Shi, M. Zhang, Z. Yang, *et al.*, "Determination of Critical Micelle Concentrations of Surfactants by Terahertz Time-Domain Spectroscopy," *IEEE Transactions on Terahertz Science & Technology,* vol. 6, pp. 532-540, 2016.

[32] S. H. Wang, "APPLICATIONS AND PROSPECTS OF TERAHERTZ TECHNOLOGY," *Physics,* 2001.

[33] K. Ahi and M. Anwar, "Developing terahertz imaging equation and enhancement of the resolution of terahertz images using deconvolution," in *SPIE Commercial + Scientific Sensing and Imaging*, 2016, p. 98560N.

[34] L. Duvillaret, F. Garet, and J. L. Coutaz, "Influence of noise on the characterization of materials by terahertz time-domain spectroscopy," *Journal of the Optical Society of America B,* vol. 17, pp. 452-461, 2000.

[35] C. D. Stoik, M. J. Bohn, and J. L. Blackshire, "Nondestructive evaluation of aircraft composites using transmissive terahertz time domain spectroscopy," *Optics Express,* vol. 16, pp. 17039-17051, 2008.

[36] J. L. Prince and J. M. Links, "Medical imaging signals and systems," *Signal,* vol. 48, pp. 69-76, 2006.

[37] S. Wietzke, C. Jansen, F. Rutz, D. M. Mittleman, and M. Koch, "Determination of additive content in polymeric compounds with terahertz time-domain spectroscopy," *Polymer Testing,* vol. 26, pp. 614-618, 2007.

[38] Z. Jin, L. Wei, H. L. Cui, C. Shi, X. Han, Y. Ma, *et al.*, "Nondestructive Evaluation of Carbon Fiber Reinforced Polymer Composites Using Reflective Terahertz Imaging," *Sensors,* vol. 16, p. 875, 2016.

[39] J. Zhang, J. Chen, J. Wang, J. Lang, J. Zhang, Y. Shen, *et al.*, "Nondestructive evaluation of glass fiber honeycomb sandwich panels using reflective terahertz imaging," *Journal of Sandwich Structures & Materials,* p. 109963621771162, 2017.

[40] A. J. Fitzgerald, S. Pinder, A. D. Purushotham, P. O'Kelly, P. C. Ashworth, and V. P. Wallace, "Classification of terahertz-pulsed imaging data from excised breast tissue," *Journal of Biomedical Optics,* vol. 17, p. 016005, 2012.

[41] L. Baldacci, M. Pagano, L. Masini, A. Toncelli, G. Carelli, P. Storchi, *et al.*, "Non-invasive absolute measurement of leaf water content using terahertz quantum cascade lasers," *Plant Methods,* vol. 13, p. 51, 2017.

[42] Y. Wang, R. C. Fang, M. M. Lin, L. U. Yan, L. Wang, and B. Jin, "Anatomical Structure Dynamics of Ginkgo biloba L. Leaves during Annual Growth and Development," *Acta Botanica Boreali-Occidentalia Sinica,* vol. 31, pp. 942-949, 2011.

[43] H. Lambers, F. S. C. Iii, and T. L. Pons, *Plant physiological ecology*: Springer, 2008.

[44] L. Qin and W. Fang, "Study on the comparative anatomy of the leaves of 16 bamboo species in China," *Journal of bamboo research,* vol. 5, pp. 78-86, 1986.

[45] T. Kirsch, F. Kaffarnik, M. Riederer, and L. Schreiber, "Cuticular permeability of the three tree species Prunus laurocerasus L., Ginkgo biloba L. and Juglans regia L.: comparative investigation of the transport properties of intact leaves, isolated cuticles and reconstituted cuticular waxes," *Journal of Experimental Botany,* vol. 48, pp. 1035-1045, 1997.

[46] T. J. K. Dilks and M. C. F. Proctor, "Photosynthesis, Respiration and Water Content in Bryophytes," *New Phytologist,* vol. 82, pp. 97-114, 1979.

[47] L. Chaerle and D. S. D. Van, "Imaging techniques and the early detection of plant stress," *Trends in Plant Science,* vol. 5, p. 495-501, 2000.

[48] J. M. Clarke, I. Romagosa, S. Jana, J. P. Srivastava, and T. N. Mccaig, "Relationship of excised-leaf water loss rate and yield of durum wheat in diverse environments," *Canadian Journal of Plant Science,* vol. 69, pp. 1075-1081, 1989.

[49] P. Lai, L. Wang, J. W. Tay, and L. V. Wang, "Photoacoustically guided wavefront shaping for enhanced optical focusing in scattering media," Nature Photonics, vol. 9, no. 2, pp. 126-132, 2015.

[50] Z. Yu, H. Li, and P. Lai, "Wavefront Shaping and Its Application to Enhance Photoacoustic Imaging," Applied Sciences, vol. 7, no. 12, p. 1320, 2017.

Figure captions:

Fig. 1. Visible optical images of leaves (a) wintersweet, (b) ginkgo, and (c) bamboo.

Fig. 2. (a) Schematic diagram of a typical THz-TDS setup. (b) Physical diagram of the THz-TDS system in the transmission mode. The measured sample was fixed on the XY two-dimensional moving stage for imaging.

Fig. 3. Time-domain peak-to-peak imaging (a) and frequency-domain imagings at 0.6 THz (b), 0.89 THz (c), and 1.15 THz (d) of the winntersweet leaf in the fourth day.

Fig. 4. Frequency-domain imagings of wintersweet (a), ginkgo (b), and bamboo (c) at the optimal frequency in seven successive days.

Fig. 5. Variations of THz image signals with drying days at the distal, intermedial and basal regions of different leaves. (a) wintersweet; (b) ginkgo; (c) bamboo.

Fig. 6. Variations of THz image signals with drying days at different regions for different parts of the wintersweet leaf. (a) main vein; (b) lateral vein; (c) mesophyll.

Fig. 7. Water content of wintersweet, ginkgo and bamboo leaves measured by the weighing method.

Fig. 8. Correlation between THz image signals and gravimetric water content for wintersweet (a), ginkgo (b), and bamboo (c) with the linear regression fitting line and the Pearson correlation coefficient.

Fig. 9. Variations of THz transmission amplitude with the region of the control (a) and damaged (b) ginkgo leaves on the first and seventh days.

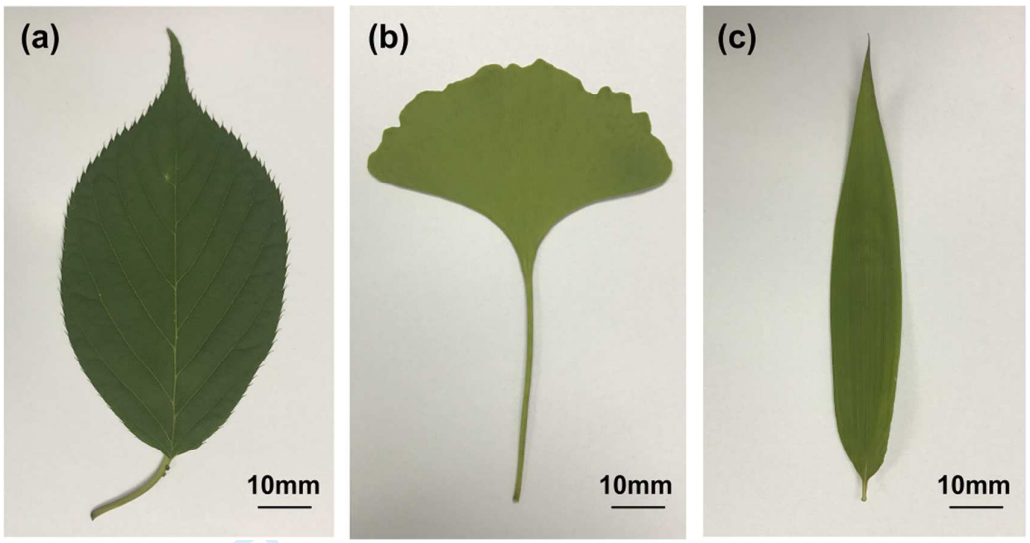

Figure. 1

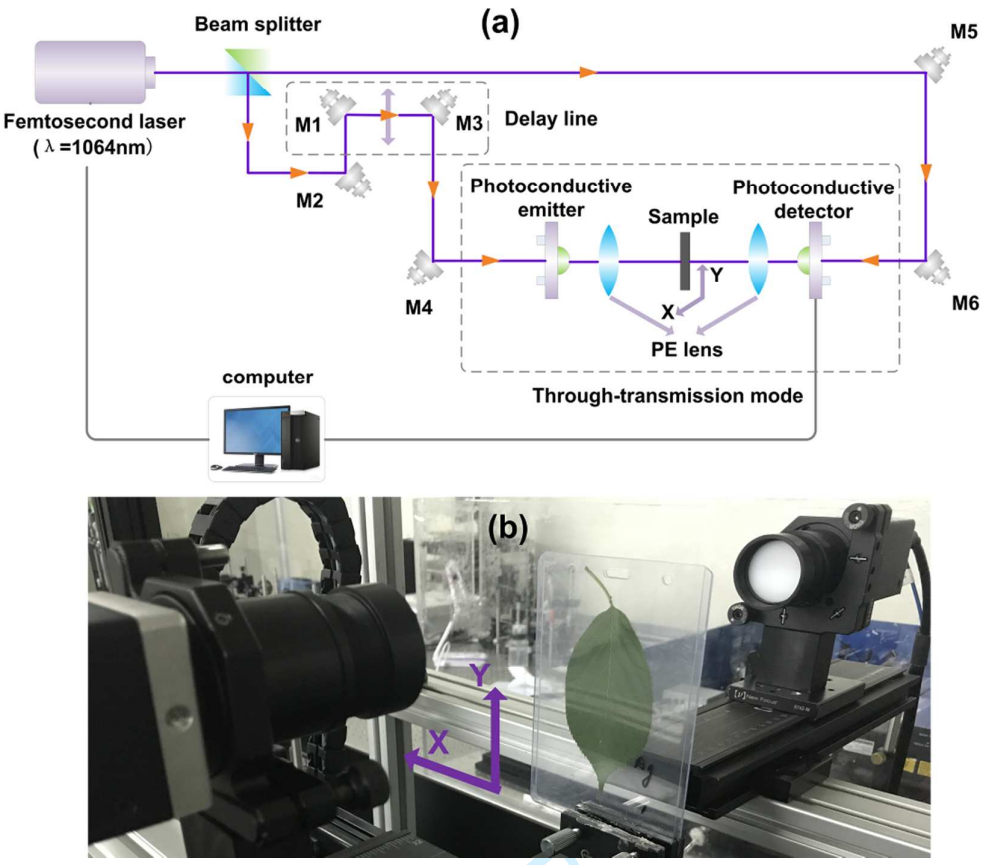

Figure. 2

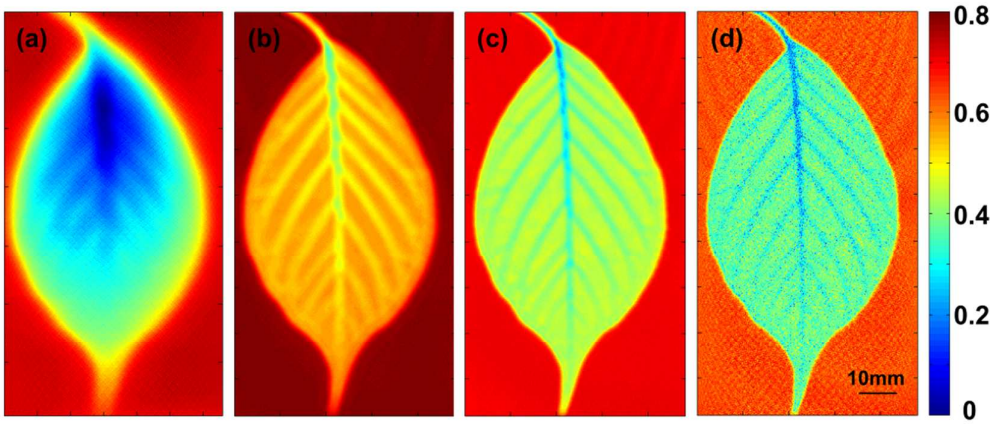

Figure. 3

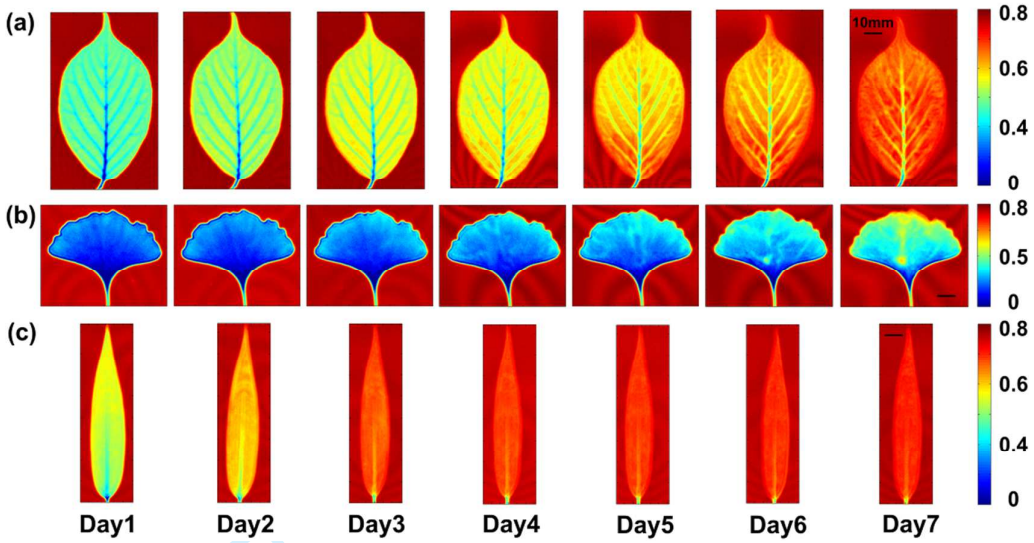

Figure. 4

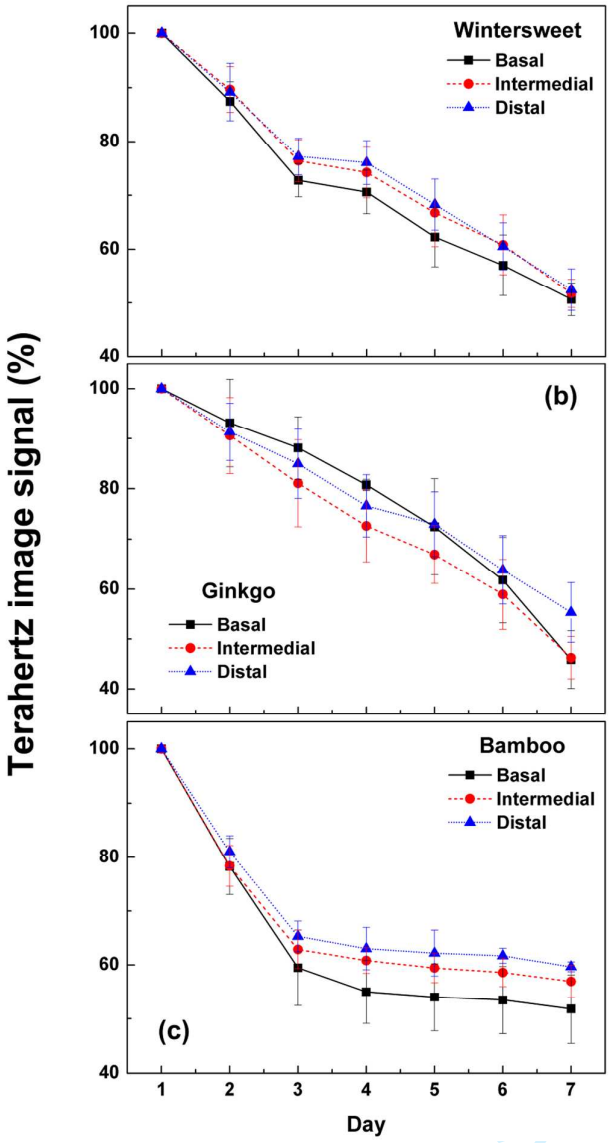
Terahertz image signal (%)
Wintersweet
Basal
Intermedial
Distal
(b)
Ginkgo
Basal
Intermedial
Distal
Bamboo
Basal
Intermedial
Distal
(c)
100
80
60
40
1
2
3
4
5
6
7
Day

Figure. 5

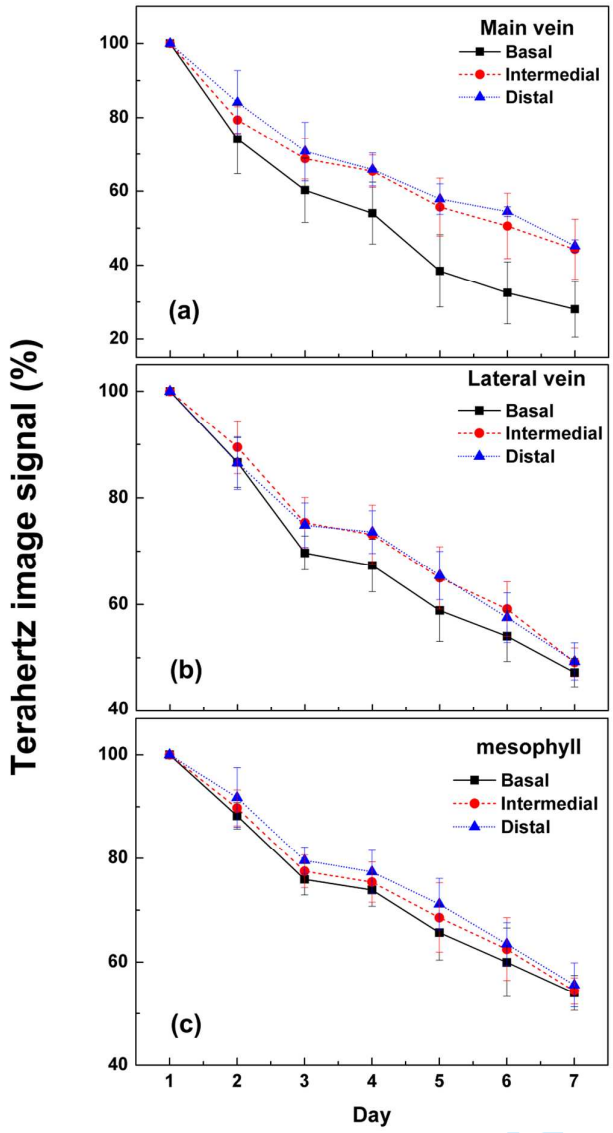
Terahertz image signal (%)
Main vein
Basal
Intermedial
Distal
(a)
Lateral vein
Basal
Intermedial
Distal
(b)
mesophyll
Basal
Intermedial
Distal
(c)
100
80
60
40
20
1
2
3
4
5
6
7
Day

Figure. 6

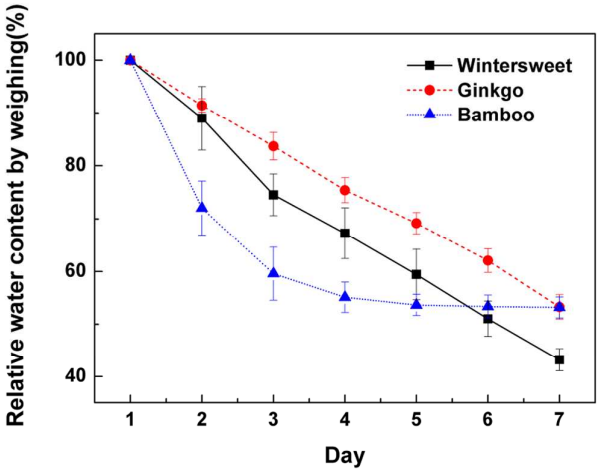

Figure. 7

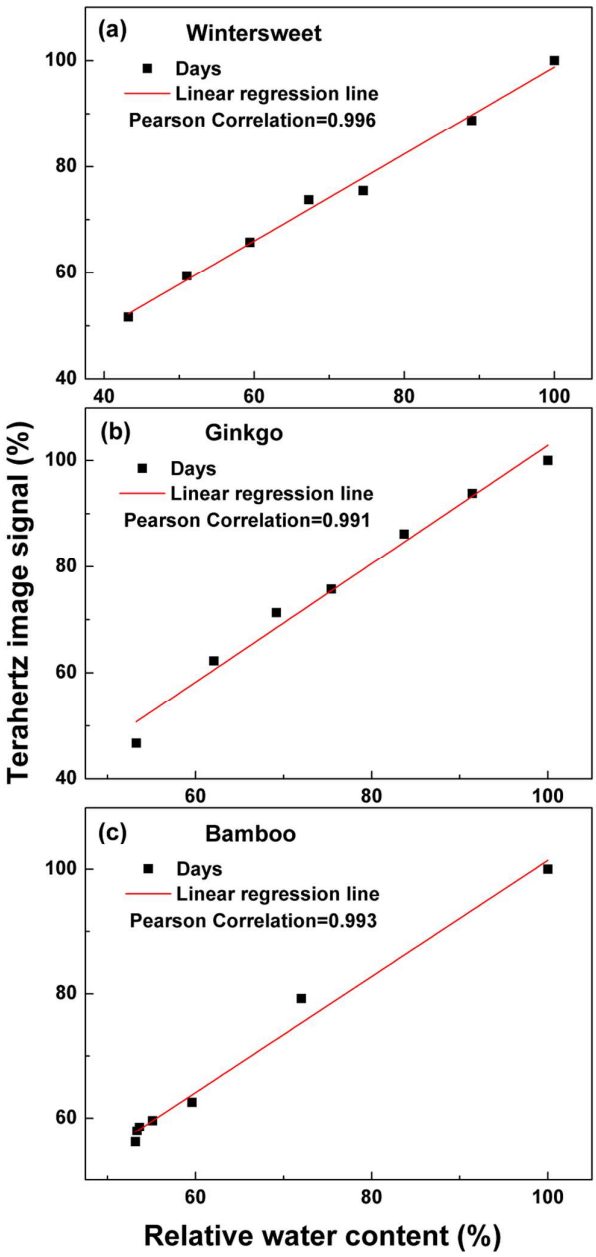
(a)
Wintersweet
Days
Linear regression line
Pearson Correlation=0.996
(b)
Ginkgo
Days
Linear regression line
Pearson Correlation=0.991
(c)
Bamboo
Days
Linear regression line
Pearson Correlation=0.993
Terahertz image signal (%)
Relative water content (%)

Figure. 8

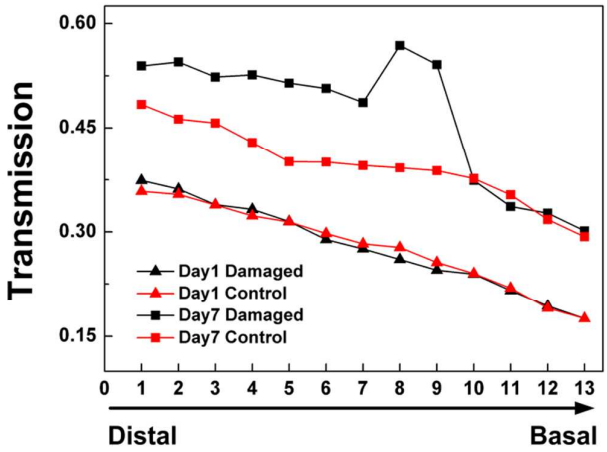

Figure. 9